

SOFT QCD RESULTS FROM ATLAS AND CMS

CLAUDIA-ELISABETH WULZ, for the ATLAS and CMS Collaborations
*Institute of High Energy Physics of the Austrian Academy of Sciences,
Nikolsdorfergasse 18, 1050 Vienna, Austria*

The ATLAS and CMS Collaborations have measured properties of minimum bias events and have determined characteristics of the underlying event in proton-proton collisions at three LHC centre-of-mass energies. Comparisons to common phenomenological models and partially to other experiments have been made. The production of the strange particles K_S^0 , Λ and Ξ is discussed. Particle correlation studies, in particular Bose-Einstein as well as long- and short-range angular correlations in proton-proton and lead ion events are explained.

1 Properties of minimum bias events

Ideally minimum bias events are those recorded with a totally inclusive trigger. The exact definition depends on the experiment. Usually minimum bias only refers to non-single-diffractive (NSD) events. In ATLAS¹ and CMS² similar minimum bias trigger detectors are used. ATLAS has two stations of Minimum Bias Trigger Scintillators (MBTS) located upstream and downstream at $z = \pm 3.56$ m from the nominal collision vertex in the pseudorapidity intervals $2.09 < |\eta| < 2.82$ and $2.82 < |\eta| < 3.84$. CMS has Beam Scintillator Counters (BSC) at $z = \pm 10.86$ m within $3.23 < |\eta| < 4.65$. Both experiments also use signals from a beam pick-up based timing system (BPTX) at $z = \pm 175$ m with a time resolution of 200 ps in their minimum bias trigger.

Transverse momentum spectra of charged particles have been measured in a large range of p_T . Fig. 1 shows results from the CMS experiment and comparisons to CDF data³. Calorimeter-based transverse energy triggers have been used in the high- p_T -region instead of the normal minimum bias trigger. The data are fully corrected. The inclusive invariant cross-section expressed as a function of the scaling variable $x_T = 2p_T/\sqrt{s}$ is given by Eq. 1.

$$E \frac{d^3\sigma}{dp^3} = F(x_T)/p_T^{n(x_T, \sqrt{s})} = F'(x_T)/\sqrt{s}^{n(x_T, \sqrt{s})} \quad (1)$$

Minimum bias pseudorapidity and multiplicity distributions as measured by ATLAS⁴ are depicted in Fig. 2. The rapidity plateau extends to $|\eta| \approx 1$ for both centre-of-mass energies of 0.9 and 7 TeV, however, there is an increase of almost a factor of two in its height. No Monte Carlo tune describes the multiplicity distribution shown in Fig. 2c well.

2 Underlying event studies

The underlying event (UE) comprises all particles except those from a given hard interaction of interest. It has components from multiple semi-hard parton scattering processes and soft

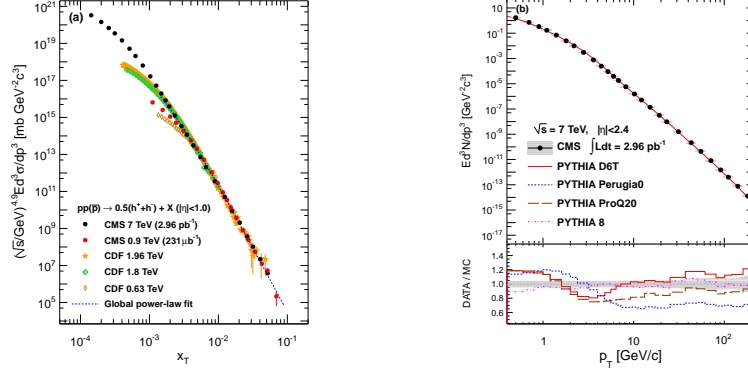


Figure 1: x_T scaling curves (a), inclusive invariant cross-section (b)

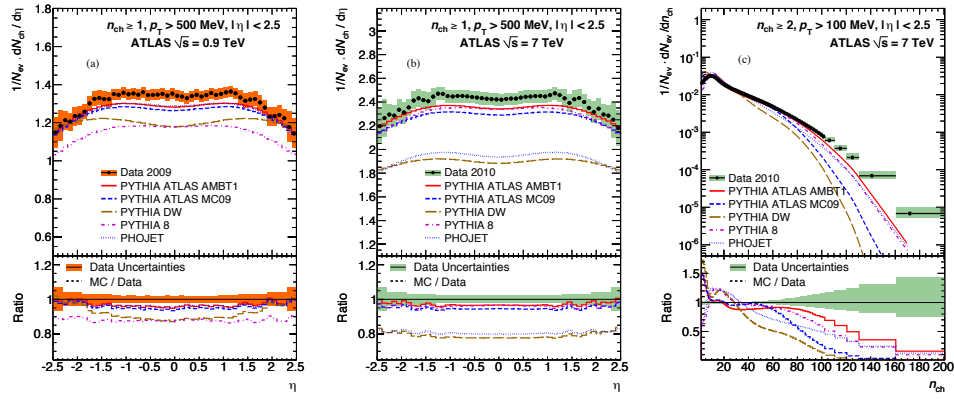


Figure 2: Minimum bias pseudorapidity distributions at $\sqrt{s} = 0.9$ TeV (a) and 7 TeV (b), multiplicity distribution at $\sqrt{s} = 7$ TeV (c)

components from beam-beam remnants. The dominant momentum flow defines three regions in the plane transverse to the incoming beams. It is given by the direction of the highest- p_T track in ATLAS, whereas in CMS the leading track jet is used instead. The region within an azimuthal angle difference of $|\Delta\phi| < 60^\circ$ with respect to the leading object is called the toward region, and the one opposite ($|\Delta\phi| > 120^\circ$) the away region. The area in between, the transverse region, is the one that is most sensitive to the UE.

ATLAS⁵ and CMS⁶ measured various properties of charged particles in the UE such as multiplicity and transverse momentum distributions. Multiplicity and Σp_T densities as a function of the leading- p_T entity were also studied. There is a strong growth of UE activity with \sqrt{s} .

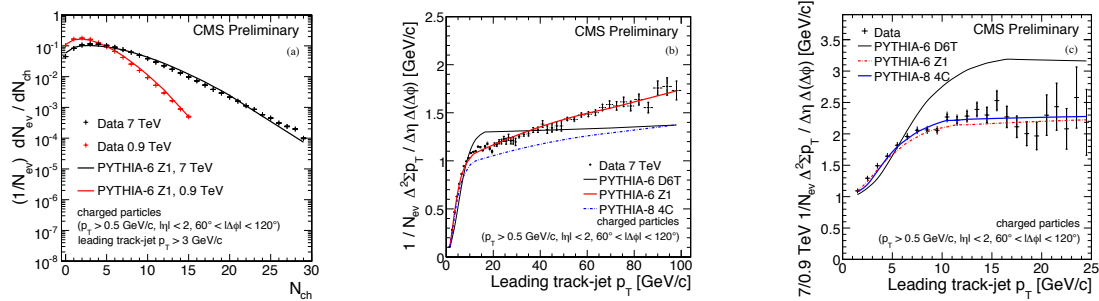


Figure 3: Underlying event multiplicities (a), average scalar momentum sum (b), multiplicity density ratio (c)

Fig. 3a shows the increase of the number of events for centre-of-mass energies from 0.9 to 7 TeV

as a function of multiplicity for the transverse region. The average scalar momentum sum rises sharply till 8 GeV due to the increase of multiple parton interaction activity, followed by a slow increase thereafter (Fig. 3b). The distributions in Fig. 3 are well reproduced by the PYTHIA Z1 Monte Carlo tune ⁷.

The charged particle multiplicity density in the transverse region is plotted in Fig. 4a. Compared to minimum bias there is about two times more activity in the UE. All Monte Carlo models underestimate the multiplicity. Figs. 4b and 4c show the increase of the UE p_T by about 20% from 0.9 to 7 TeV, well reproduced by a variety of models.

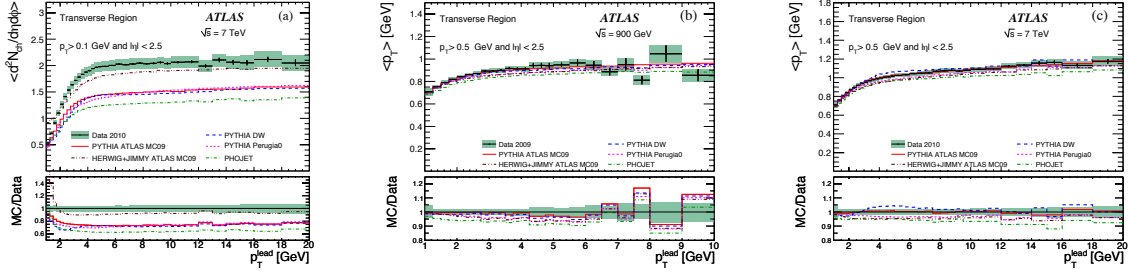


Figure 4: Charged particle multiplicity density (a), average transverse momentum at $\sqrt{s} = 900$ GeV (b) and 7 TeV (c)

3 Strangeness production

The production of the strange hadrons K_S^0 , Λ and Ξ has been studied ⁸. The mass peaks have been reconstructed, as shown in Fig. 5a for the Ξ^- . Production rates have been measured as functions of rapidity and transverse momentum. The p_T distributions extend from practically zero to 10 GeV for K_S^0 (Fig. 5b) and 6 GeV for Ξ^- . The increase in production of strange particles from 0.9 to 7 TeV is approximately consistent with results for charged particles described above, but the rates exceed the predictions by up to a factor of three (Fig. 5c). This deficiency probably originates from parameters regulating the frequency of s-quarks appearing in color strings.

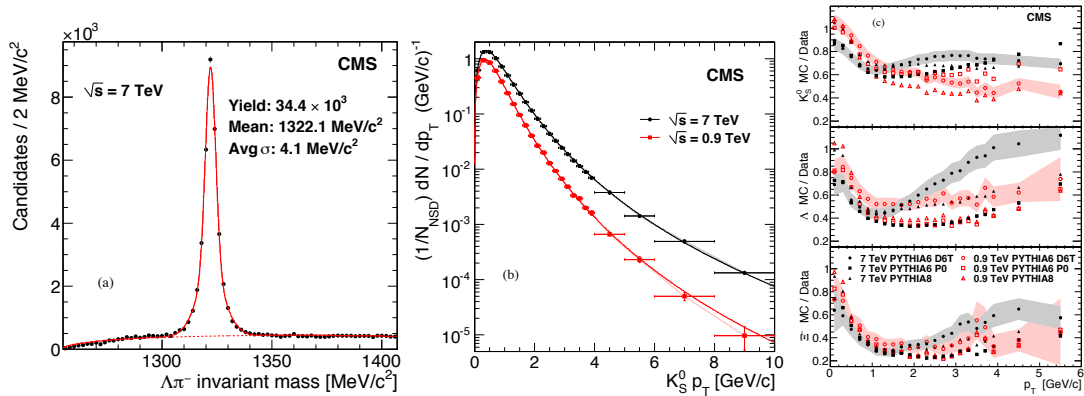


Figure 5: Ξ^- mass peak (a), p_T distribution of K_S^0 (b), hyperon p_T yield ratios (c)

4 Particle correlations

Pairs of same-sign charged particles with four-momentum difference Q in the region $0.02 \text{ GeV} < Q < 2 \text{ GeV}$ are analysed to study Bose-Einstein correlations ⁹. The radius of the effective

space-time region emitting bosons with overlapping wave functions increases with multiplicity, whereas the correlation strength decreases. Both decrease with increasing momentum difference k_T . Anticorrelations between same-sign charged particles are observed for Q values above the signal region, which can be seen in Fig. 6c showing the double ratio $R(Q)^{10}$.

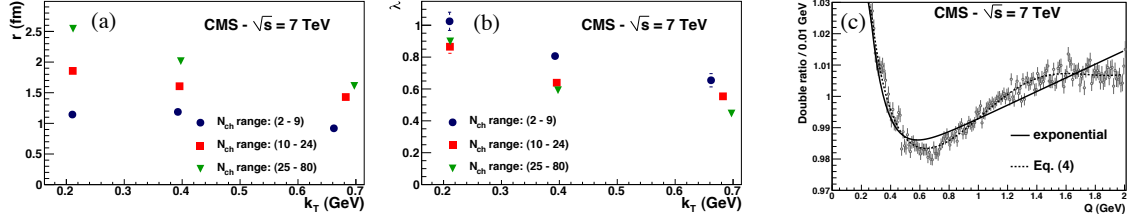


Figure 6: Radius r (a), correlation strength λ (b), double ratio showing anticorrelations (c)

Near-side long-range particle correlations in proton data have first been reported by CMS¹¹. A ridge, a pronounced structure in high-multiplicity events for rapidity and azimuth differences of $2.0 < |\Delta\eta| < 4.8$ and $\Delta\phi \approx 0$ has been found. Long- and short-range correlations in ion data have also been studied¹². The correlation functions of the 0-5% most central collisions show characteristic features not present in minimum bias proton interactions (Fig. 7). The ridge is most evident for p_T 's of the trigger particle between 2 and 6 GeV, but disappears at high p_T .

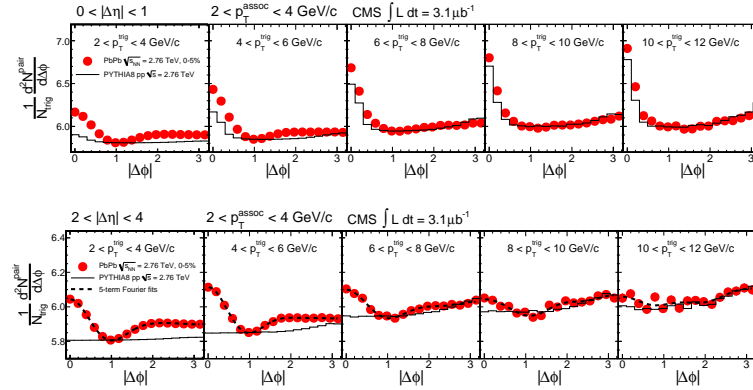


Figure 7: Short-range ($0 < |\Delta\eta| < 1$) and long-range ($2 < |\Delta\eta| < 4$) correlations in lead ion data

References

1. ATLAS Collaboration, *JINST* **3**, S08003 (2008).
2. CMS Collaboration, *JINST* **3**, S08004 (2008).
3. CMS Collaboration, arXiv:1104.3547, submitted to *J. High Energy Phys.*
4. ATLAS Collaboration, arXiv:1012.5104, accepted by *New J. Phys.*
5. ATLAS Collaboration, arXiv:1012.0791, submitted to *Phys. Rev. D*
6. CMS Collaboration, CMS-QCD-10-010.
7. R. Field, arXiv:1010.3558.
8. CMS Collaboration, arXiv:1102.4282, *J. High Energy Phys.* **05**, 064 (2011).
9. CMS Collaboration, arXiv:1101.3518, accepted by *J. High Energy Phys.*
10. T. Csörgő, W. Kittel, W. J. Metzger, T. Novák, *Phys. Lett. B* **663**, 214 (2011).
11. CMS Collaboration, arXiv:1009.4122, *J. High Energy Phys.* **09**, 091 (2010).
12. CMS Collaboration, arXiv:1105.2438, submitted to *J. High Energy Phys.*